Available online at www.sciencedirect.com
ScienceDirect
Journal of Magnetism and Magnetic Materials 321 (2009) 971–973
Journal of magnetism and magnetic materials
www.elsevier.com/locate/jmmm

Magneto-optical and micromagnetic simulation study of the current-driven domain wall motion in ferromagnetic (Ga,Mn)As

K.Y. Wang[a,*], A.C. Irvine[b], R.P. Campion[c], C.T. Foxon[c], J. Wunderlich[a], D.A. Williams[a], B.L. Gallagher[c]

[a]Hitachi Cambridge Laboratory, Madingley Road, Cambridge CB3 0HE, UK
[b]Cavendish Laboratory, Microelectronics Research Centre, University of Cambridge, Cambridge CB3 0HE, UK
[c]School of Physics and Astronomy, University of Nottingham, Nottingham NG7 2RD, UK

Available online 19 March 2008

Abstract

We have studied current-driven domain wall motion in modified $Ga_{0.95}Mn_{0.05}As$ Hall bar structures with perpendicular anisotropy by using spatially resolved polar magneto-optical Kerr effect microscopy and micromagnetic simulation. Regardless of the initial magnetic configuration, the domain wall propagates in the opposite direction to the current with critical current of $1–2 \times 10^5$ A/cm^2. Considering the spin-transfer torque term as well as various effective magnetic field terms, the micromagnetic simulation results are consistent with the experimental results. Our simulated and experimental results suggest that the spin-torque rather than Oersted field is the reason for current-driven domain wall motion in this material.
© 2008 Elsevier B.V. All rights reserved.

Keywords: Spin-torque; Magneto-optical; Micromagnetic

1. Introduction

Manipulation of magnetization and the magnetic domain wall motion using spin-polarized current has attracted much attention for potential applications in spintronics, such as novel magnetic devices using written information with an electrical current. The spin-polarized current gives the angular momentum to the local magnetization, which is called the spin-transfer torque [1]. Current driven domain wall motion in both the ferromagnetic metals and magnetic semiconductors has been demonstrated, although the mechanism is still in debate [2–4]. The critical current density for domain wall motion is predicted to be proportional to the saturation magnetization [5,6]. In diluted magnetic semiconductor (Ga,Mn)As doped with Mn 1–10%, the saturation magnetization is one to two orders of magnitude smaller than that of the metallic ferromagnets. (The experimentally observed critical current for ferromagnetic semiconductor (Ga,Mn)As is 1–2 orders of magnitude smaller than that in ferromagnetic metals [7].) The lower electrical current, the heating effect and the Oersted field produced by the electrical current are weaker. Because of the low critical current density, a ferromagnetic semiconductor is one of the best candidates for understanding current-driven domain wall motion. In this letter, we use polar magneto-optical Kerr microscopy (PMOKM) and LLG micromagnetic simulations [8] to study the current-driven domain wall motion in $Ga_{0.95}Mn_{0.05}As$ modified Hall bar devices.

2. Experimental results

25 nm (Ga,Mn)As epilayers grown on a relaxed (0 0 1) (In,Ga)As buffer layer experience a tensile strain due to the difference in the lattice constant in each layer. Under these growth conditions, the magnetic easy axis is known to be perpendicular to the growth plane in agreement with the theory. Magnetic domain patterns in the (Ga,Mn)As thin films have been studied previously using PMOKM [9]. During the magnetic reversal, in-situ imaged domain patterns clearly show that the domain walls are nucleated and propagate along the film. It suggests that we can easily

*Corresponding author. Tel.: +44 1223 442933; fax: +44 1223 467942.
E-mail address: kw301@cam.ac.uk (K.Y. Wang).

0304-8853/$ - see front matter © 2008 Elsevier B.V. All rights reserved.
doi:10.1016/j.jmmm.2008.03.022

make use of the nucleated domain walls for studying current-driven domain wall motion in these materials. A 4 μm wide modified Hall bar device was fabricated with electron beam lithography, as shown in Fig. 1. The length between the two neighbouring arms along the bar is 20 μm and the total length of the bar is 120 μm. A 10 nm surface layer has been etched away at the both ends, as shown in Fig. 1. Due to the different coercive field for the etched and non-etched part of the devices, we initialize two domain walls at both interfaces by an external magnetic field. No matter what the relation between the applied current direction and domain wall motion direction is, we expect to see the domain wall motion under the Kerr microscopy image window.

Initially, the device is saturated with a negative magnetic field $H = -300$ Oe, which is much higher than the coercive field. The field is then swept to $H = 45$ Oe, which only switches part of the device with the two domain walls formed at the interface. The image of the initial magnetic configuration is shown in Fig. 2a. During the application of the dc current, we screen the light in order to prevent the complication of light-excited effects. Increasing dc current from zero to negative value at a rate of 2×10^4 A/cm^2 s, we monitor the Hall resistance for both the *A* and *B* arm pairs simultaneously. Large anisotropic magnetoresistance and anomalous Hall effect was observed in GaMnAs devices because of strong spin–orbit coupling [10]. The anomalous Hall effect is very sensitive to the local magnetization. When we observe an abrupt change of the Hall resistance, we switch the dc current to zero. The monitored Hall resistances for A and B arm pairs are shown in Fig. 2b. The longitudinal resistance increases by about 3% during the applied dc current. Compared with the temperature dependence of the longitudinal resistance measured at low current density $j = 1 \times 10^3$ A/cm^2, the temperature rise because of heating during the applying dc current is less than 10 K. The magnetic configuration image after applying the dc current of Fig. 2b is shown in Fig. 2c. The right side domain wall propagates about 60 μm along the channel to the left side. The direction of motion is opposite to the electrical current direction with critical current $\sim$1–2 $\times 10^5$ A/cm^2. Regardless of the initial magnetic configuration, we find that the domain wall motion

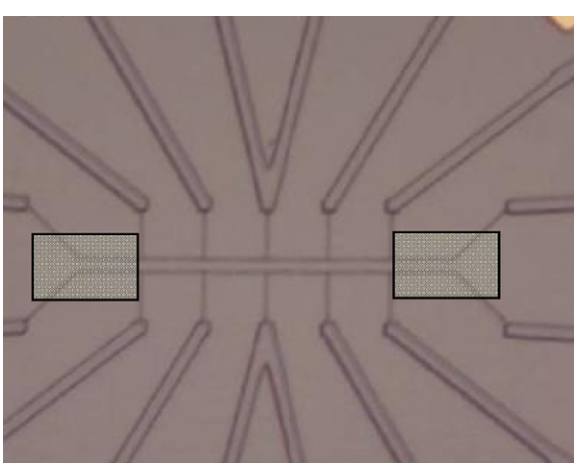

Fig. 1. The fabricated modified multi-arms Hall bar device with a width of 4 μm and the length between the neighbouring arms 20 μm. The surface of the two square marked parts has been etched away about 10 nm.

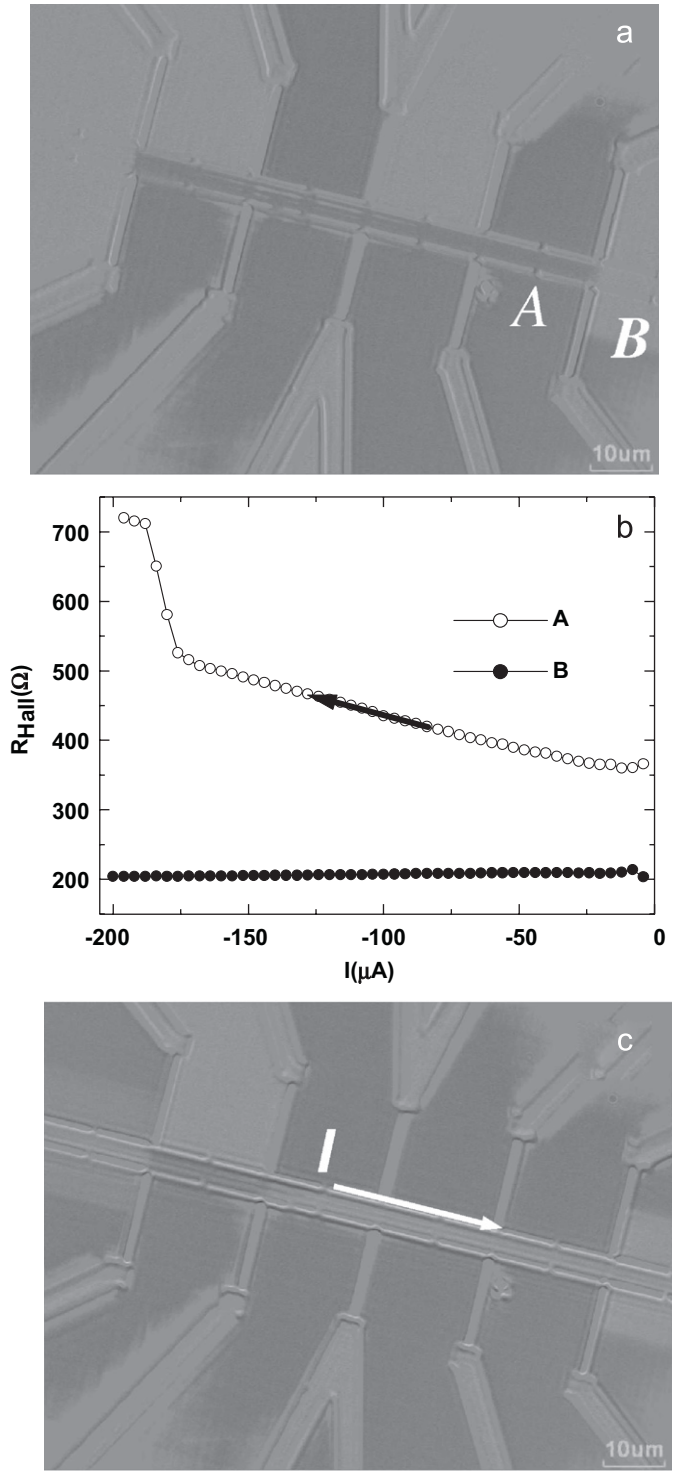

Fig. 2. (a) Initial magnetic configuration with domain wall at both sides. (b) The in-situ monitored Hall resistance at bar *A* and *B* while applying dc current. (c) Final magnetic configuration after applying dc current. The domain wall motion direction is opposite to the electrical current direction.

direction is always opposite to the electrical current direction, which is in agreement with other experiments [4,7]. The heating effect has no preferred direction. If the current generated Oersted field is the origin of the domain wall motion, the domain wall motion direction should be sensitive to the initial magnetic configuration. It shows that the spin-transfer torque rather than the heating effect and the Oersted field is the origin of the current driving domain wall motion. The relation between the current direction and domain wall motion can be explained by the fact that because (Ga,Mn)As is a p-type conductor the electrical current and the carriers move in the same direction. The interaction between the itinerate holes and localized Mn spins is p–d antiferromagnetic coupling [11]. The spin-polarized holes give the momentum to the localized magnetization. The domain wall motion direction is expected to be opposite to the current direction, which is in agreement with the observed results.

3. Micromagnetic simulations

In this section, the micromagnetic simulations were carried out to study the current-driven domain wall in a GaMnAs slab with the physical dimensions 5200 nm length, 640 nm width and 20 nm thickness. The Gilbert damping constant $\alpha = 0.02$ [12], the magnetic anisotropy constant $K_U = 2 \times 10\,\mathrm{J/m^3}$ and saturation magnetization $M_S = 25\,\mathrm{emu/cm^3}$ are used. The initial magnetic state with one stable domain wall is shown in Fig. 3a. We have simulated the current-driven domain wall motion at different current densities with other simulated parameters fixed. The magnetic configuration after applying 6 ns dc current is shown in Fig. 3b–d. The critical current density for the domain wall motion is $2.5 \times 10^5\,\mathrm{A/cm^2}$, which is only 1–2 times larger than that of the experimental results. The domain wall displacement increases with increasing applied current density. The domain wall is still quite sharp and clean at low current density and distorted by the Oersted field at high current density. The distortion of the domain wall from Oersted field is underestimated here, because we have not considered the Oersted field generated by the anomalous Hall field [7]. The simulated results also show convincingly that the spin-torque is the origin of the current driving domain wall motion. In the simulation, we have not considered the non-adiabatic term and the heating effect from the electrical current for the current driving domain wall. We will study this in more detail elsewhere.

4. Conclusions

Combining experimental PMOKM measurements and micromagnetic simulations, we have studied the current-driven domain wall motion in modified $Ga_{0.95}Mn_{0.05}As$ Hall bar devices. The domain wall always moves in opposite direction to the current independent of the initial magnetic configuration. The critical current density obtained from the experiments is $1–2 \times 10^5\,\mathrm{A/cm^2}$, which is in agreement with the simulated results.

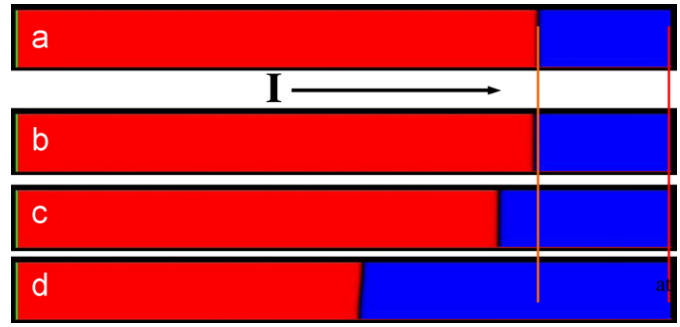

Fig. 3. Micromagnetic simulation results: (a) initial magnetic configuration; magnetic configuration after applying dc current 6 ns with current density (b) $J = 2.5 \times 10^5\,\mathrm{A/cm^2}$; (c) $J = 2 \times 10^6\,\mathrm{A/cm^2}$ and (d) $J = 1 \times 10^7\,\mathrm{A/cm^2}$. Arrow points to the electrical current direction.

Acknowledgements

This project was supported by EC sixth framework Grant No. FP6-IST-015728 and EPSRC-GB(GR/S81407/01).

References

[1] L. Berger, Phys. Rev. B 54 (1996) 9353;
J. Slonczewski, J. Magn. Magn. Mater. 159 (1996) L1.
[2] A. Fert, V. Cros, J.M. George, J. Grollier, H. Jaffrès, A. Hamzic, A. Vaurès, G. Faini, J.B. Youssef, H. LeGall, J. Magn. Magn. Mater. 272 (2004) 1706.
[3] M. Hayashi, L. Thomas, C. Rettner, R. Moriya, Stuart S.P. Parkin, Nat. Phys. 3 (2007) 21.
[4] M. Yamanouchi, D. Chiba, F. Matsukura, H. Ohno, Nat.(London) 428 (2004) 539.
[5] S. Zhang, Z. Li, Phys. Rev. Lett. 93 (2004) 127204.
[6] G. Tatara, H. Kohno, Phys. Rev. Lett. 92 (2004) 086601.
[7] M. Yamanouchi, D. Chiba, F. Matsukura, T. Dietl, H. Ohno, Phys. Rev. Lett. 96 (2006) 096601.
[8] http://llgmicro.home.mindspring.com/.
[9] K.Y. Wang, A.W. Rushforth, V.A. Grant, R.P. Campion, K.W. Edmonds, C.T. Foxon, B.L. Gallagher, J. Wunderlich, D.A. Williams, J. Appl. Phys. 101 (2007) 106101.
[10] K.Y. Wang, K.W. Edmonds, R.P. Campion, L.X. Zhao, C.T. Foxon, B.L. Gallagher, Phys. Rev. B 72 (2005) 085201.
[11] T. Dietl, H. Ohno, F. Matsukura, Phys. Rev. B 63 (2001) 195205.
[12] J. Sinova, T. Jungwirth, X. Liu, Y. Sasaki, J.K. Furdyna, W.A. Atkinson, A.H. MacDonald, Phys. Rev. B 69 (2004) 085209.